Available online at www.sciencedirect.com
SCIENCE DIRECT®
Thermochimica Acta 419 (2004) 1–17
thermochimica acta
www.elsevier.com/locate/tca

Review

Isothermal reaction calorimetry as a tool for kinetic analysis

Andreas Zogg, Francis Stoessel, Ulrich Fischer*, Konrad Hungerbühler

ETH Zurich, ICB, Safety and Environmental Technology Group, ETH Hoenggerberg, HCI G137, 8093 Zurich, Switzerland

Received 14 November 2003; received in revised form 14 January 2004; accepted 16 January 2004

Available online 17 March 2004

Abstract

Reaction calorimetry has found widespread application for thermal and kinetic analysis of chemical reactions in the context of thermal process safety as well as process development. This paper reviews the most important reaction calorimetric principles (heat-flow, heat-balance, power-compensation, and Peltier principle) and their applications in commercial or scientific devices. The discussion focuses on the different dynamic behavior of the main calorimetric principles during an isothermal reaction measurement. Examples of available reaction calorimeters are further compared considering their detection limit, time constant as well as temperature range.

In a second part, different evaluation methods for the isothermally measured calorimetric data are reviewed and discussed. The methods will be compared, focusing especially on the fact that reaction calorimetric data always contains additional informations not directly related to the actual chemical reaction such as heat of mixing, heat of phase-transfer/change processes or simple measurement errors. Depending on the evaluation method applied such disturbances have a significant influence on the calculated reaction enthalpies or rate constants.

Keywords: Reaction calorimetry; Kinetics; Thermal analysis; Heat-flow; Heat-balance; Power-compensation; Peltier

1. Introduction

Kinetic and thermodynamic characterization of chemical reactions is a crucial task in the context of thermal process safety as well as process development [1]. As most chemical and physical processes are accompanied by heat effects calorimetry represents a unique technique to gather informations about both aspects, thermodynamics as well as kinetics. As the heat-flow rate during a chemical reaction is proportional to the rate of conversion (mol/s), calorimetry represents a differential kinetic analysis method [2]. This can be expressed in terms of the following mathematical expression:

$$\dot{q}_{\mathrm{React}}(t) \sim r(t) V_{\mathrm{r}} \tag{1}$$

where $\dot{q}_{\mathrm{React}}$ is the reaction heat-flow rate (W), determined by a calorimeter, r the rate of reaction (mol/m^3/s), and V_{r} the reaction volume (m^3). All the three variables $\dot{q}_{\mathrm{React}}$, r, and V_{r} are a function of time and reaction progress and thus, change during a reaction measurement. In contrast to calorimetry most of the other analytical techniques applied in the context of kinetic analysis, such as concentration measurements, online measurement of reaction spectra (UV-Vis, near infrared, mid infrared, Raman ...) can be compared to integral kinetic analysis methods [2]. This can be expressed in terms of the following proportionality:

$$s_i(t) \sim c_i(t) \tag{2}$$

where s_i represents the values measured by one of the analytical sensors mentioned above corresponding to the ith component in the reaction system with the concentration profile $c_i(t)$ (mol/m^3). From this consideration it becomes clear that any combination of a differential analysis method, such as calorimetry, with an integral analysis method might lead to a significant improvement of the kinetic analysis [3]. In the second part of this paper, some of these combined evaluation techniques will be presented.

In a first part of this paper, we will give an overview on the different calorimetric principles applied. However, the review will be restricted to reaction calorimeters that resemble the later production-scale reactors of the corresponding industrial processes (batch or semi-batch reactors). This paper will not discuss, thermal analysis devices such as differential scanning calorimeter (DSC) or other micro calorimetric devices that differ significantly from the production-scale reactor.

* Corresponding author. Tel.: +41-16325668; fax: +41-16321189.
E-mail address: ufischer@tech.chem.ethz.ch (U. Fischer).

0040-6031/$ – see front matter © 2004 Elsevier B.V. All rights reserved.
doi:10.1016/j.tca.2004.01.015

For the purpose of scale-up as well as kinetic and thermodynamic analysis of a desired synthesis reaction, isothermal reaction measurements are mostly preferred. Therefore, this review will focus on isothermal reaction calorimetric measurements. However, it should be mentioned that especially in the field of safety analysis mainly non isothermal measurements are carried out in order to investigate undesired decomposition reactions. Since non isothermal experiments contain information about the temperature dependency of the investigated chemical reaction system, their information content is obviously larger, compared to an isothermal measurement. This may be an advantage when sophisticated evaluation methods were available, but especially for complex reaction systems the information density of a non isothermal reaction measurement often gets too large for the common analysis methods. In addition, isothermal conditions also present the advantage that the signals obtained from additional integral analytical sensors, which may be combined with the calorimetric measurement will, not be affected by their temperature dependency. Thus, the field of non isothermal analysis will not be discussed here.

Reviews on the principles and the development of different types of reaction calorimeters were already presented by several authors [4–7]. A rather general overview about calorimetry is given by Hemminger and Höhne [8]. This paper will focus on the dynamic behavior of the different types of reaction calorimeters for the general case of a reaction measurement with a changing heat-transfer coefficient on the reactor wall. Additionally a comparison of available reaction calorimeters with respect to detection limits, time constants as well as temperature range will be given.

In a second part of this publication, we will present an overview on different evaluation methods of isothermally measured calorimetric reaction data. The aim of the discussed methods is to deliver the reaction enthalpy as well as kinetic model parameters (such as rate constants or reaction orders) of the investigated chemical reaction. If several isothermal measurements at different temperatures are evaluated activation energies can also be determined.

Advantages and disadvantages of the different methods will be discussed mainly focusing on the problem that calorimetric measurements are typically affected by heat effects different to the solely reaction heat-flow rate, like phase changes or mixing effects.

2. Part 1. Reaction calorimetry

2.1. Different types of reaction calorimeters

Most of the existing reaction calorimeters consist of a reaction vessel and a surrounding jacket with a circulating fluid that transports the heat away from the reactor (see Fig. 1). Such devices can be classified according to their measurement and control principles into the following four categories:

2.1.1. Heat-flow reaction calorimeter

The temperature of the reactor-content (T_r) is controlled by varying the temperature of the cooling liquid (T_j). The heat-flow rate from the reactor-content through the wall into the cooling liquid ($\dot{q}_{Flow}$) is determined by measuring the temperature difference between reactor-content and cooling liquid. In order to convert this temperature signal into a heat-flow signal (e.g. unit Watt), a heat-transfer coefficient has to be determined using a calibration heater. To allow a fast control of the T_r, the flow rate of the cooling liquid through the jacket should be high. The heat-flow principle was developed by Regenass [9,10]. Most of the commercially used reaction calorimeters are based on the heat-flow principle, such as the RC1 from Mettler Toledo [11,12]

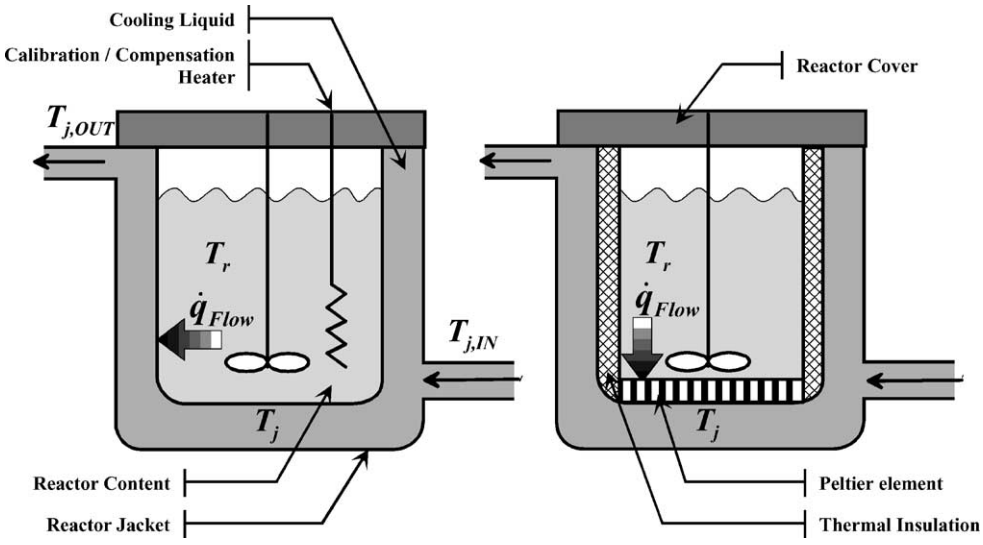

Fig. 1. Standard set-up of a reaction calorimeter. Left side: heat-flow, heat-balance, and power-compensation calorimeters. Right side: Peltier calorimeters.

(based on the work of Regenass), the SysCalo's from Systag [13] and the Simular from HEL [14,15].

2.1.2. Power-compensation reaction calorimeter

The temperature of the reactor-content (T_r) is controlled by varying the power of a compensation heating inserted directly into the reactor-content. As with an electrical heater cooling is not possible, the compensation heater always maintains a constant temperature difference between the reactor jacket and the reactor-content. Thus, "cooling" is achieved by reducing the power of the compensation heater. The heat-flow rate from the reactor-content through the wall into the cooling liquid ($\dot{q}_{Flow}$) is typically not determined because the reaction heat-flow rate is directly visible in the power consumption of the compensation heater. The temperature of the cooling liquid (T_j) is controlled at a constant temperature by an external cryostat. The power-compensation principle was first implemented by Andersen [16,17] and was further developed by Köhler et al. [18], Hentschel [19], and Schildknecht [20]. Pollard [21] and Pastré et al. [22] reported a small scale power-compensation calorimeter. Commercial power-compensation calorimeters are the AutoMate [23] and the Simular (combined with heat-flow [15]) from HEL [14].

2.1.3. Heat-balance reaction calorimeter

The temperature of the reactor-content (T_r) is controlled by varying the temperature of the cooling liquid (T_j). The heat-flow rate from the reactor-content through the wall into the cooling liquid ($\dot{q}_{Flow}$) is determined by measuring the difference between jacket inlet ($T_{j,IN}$) and outlet temperature ($T_{j,OUT}$) and the mass flow of the cooling liquid. Together with the heat capacity of the cooling liquid the heat-flow signal is directly determined without calibration. The heat-balance principle was first implemented by Meeks [24]. Commercial versions are the RM200 from Chemisens [25], the SysCalo 2000 Series from Systag [13] and the ZM-1 from Zeton Altamira [26] (developed in collaboration with Moritz and co-workers [27]).

2.1.4. Peltier calorimeters

The temperature of the reactor-content (T_r) is controlled by varying the power of the Peltier elements. In contrast to the power-compensation principle Peltier elements can be used for cooling and heating. The heat-flow rate from the reactor-content through the Peltier element into the cooling liquid ($\dot{q}_{Flow}$) is calculated based on the required electrical power and the measured temperature gradient over the Peltier elements. The temperature of the cooling liquid (T_j) is controlled at a constant temperature by an external cryostat. Becker [4,28] designed a first calorimeter using Peltier elements. A similar calorimeter was presented by Nilsson et al. [29,30] and Jansson et al. [31]. Their setup can be compared to the one shown in Fig. 1 (right side), but the whole reactor is immerged in a thermostat bath that replaces the reactor jacket. The reactor bottom consists of Peltier elements and the rest of the reactor wall is isolated. Therefore the main heat-flow out of the reactor flows through the Peltier elements. The design of Nilsson was the basis for the commercially available CPA200 from Chemisens [25]. However, in the CPA200 the heat-flow through the reactor bottom is not calculated based on the power consumption of the Peltier elements but by a heat-flow sensor which is introduced between the reactor bottom and the Peltier elements.

2.2. Different operation modes

Calorimetric applications can also be distinguished by their way of controlling the reaction temperature:

- Isothermal: T_r controlled at a constant level.
- Adiabatic: T_j controlled to avoid heat losses.
- Temperature programmed: T_r is varied according to a user defined profile.
- Isoperibole: T_j is controlled at a constant level, the reaction temperature T_r is uncontrolled.

As mentioned above this paper will only consider the isothermal operation mode. This mode is supposed to be the easiest in application because no heat accumulation by the reactor-content has to be considered. Thus, no heat capacities as a function of T_r of the reaction mixture as well as of the reactor inserts (e.g. stirrer, sensors, baffles ...) are required. However, in reality due to the non idealities of the control circuits of the calorimeters, the reaction temperature is mostly not controlled strictly isothermal. If the deviations are significant, heat accumulation terms have to be considered despite the "isothermal" operation mode.

2.3. Steady-state isothermal heat-flow balance of a general type reaction calorimeter

The only heat-flow rate considered so far is the heat-flow through the reactor jacket (Fig. 1, $\dot{q}_{Flow}$). For the general case of an isothermal reaction run the main heat-flow rates that have to be considered in a reaction calorimeter are shown in Fig. 2 and will be discussed in the following sections. The heat-flow balances will also be separately discussed for each reaction calorimeter in the following sections.

For the following discussions ideal isothermal controlling of the reaction temperature T_r will be assumed. Therefore, in Fig. 2, no heat accumulation terms of the reaction mixture and the reactor inserts are shown. However, the underlying assumption does not hold for all applications and apparatuses.

The task of the calorimeter is to determine the total heat-flow rate during a chemical reaction $\dot{q}_{tot}$ (W). Generally any kind of physical process in which heat is released or absorbed is measured. Therefore, the $\dot{q}_{tot}$ can be expressed as follows:

$$\dot{q}_{tot} = \dot{q}_{React} + \dot{q}_{Mix} + \dot{q}_{Phase} \quad (3)$$

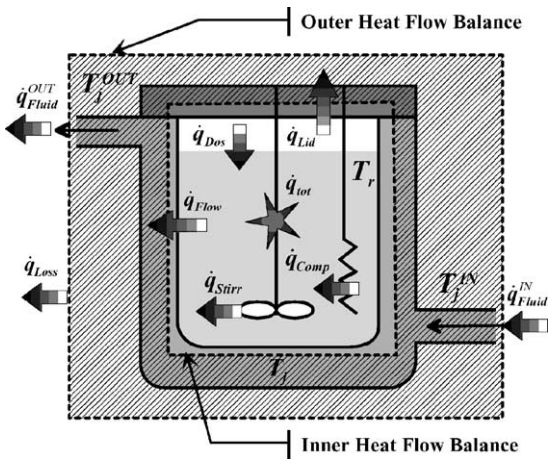

Fig. 2. Main heat-flow rates that have to be considered in a heat-flow, heat-balance, or power-compensation reaction calorimeter running at strictly isothermal conditions. The heat-flow rates inside a Peltier calorimeter are analogous (compare to Fig. 1). The direction of the heat-flow arrows corresponds to a positive heat-flow rate. For explanation of the different heat-flow rates see text.

where $\dot{q}_{\mathrm{React}}$ is the reaction heat-flow rate (W), $\dot{q}_{\mathrm{Mix}}$ the heat-flow rate occurring due to mixing enthalpies when different fluids are mixed, and $\dot{q}_{\mathrm{Phase}}$ is the heat-flow rate due to phase changes (W). For a reaction experiment at constant pressure, the reaction heat-flow rate can be further expressed as follows:

$$\dot{q}_{\mathrm{React}} = -\sum_{j=1\ldots N_{\mathrm{R}}} \Delta_r H_j r_j V_{\mathrm{r}} \tag{4}$$

where $\Delta_{\mathrm{r}}H_j$ is the enthalpy of the jth reaction (J/mol), V_{r} the volume of the reaction mixture (m^3), r_j the jth rate of reaction (mol/m^3/s) (positive sign), and N_{R} is the number of reactions.

It should be noted that in the field of reaction calorimetry the total heat-flow rate $\dot{q}_{\mathrm{tot}}$ is generally defined positive when heat is released by the chemical reaction. Therefore, a negative sign is introduced in Eq. (4) ($\dot{q}_{\mathrm{React}}$ is positive for an exothermal reaction with a negative $\Delta_{\mathrm{r}}H$).

The heat evolved by the stirrer $\dot{q}_{\mathrm{Stirr}}$ (W) can be described as follows [32]:

$$\dot{q}_{\mathrm{Stirr}} = \mathrm{Ne}\rho_{\mathrm{r}} {n_{\mathrm{S}}}^3 {d_{\mathrm{R}}}^5 \tag{5}$$

where Ne is the Newton number, ρ_{r} the density of the reaction mixture (kg/m^3), n_{S} the stirrer frequency (Hz), and d_{R} is the diameter of the stirrer (m). The heat-flow rate caused by the dosing of reactants $\dot{q}_{\mathrm{Dos}}$ (W) can be expressed as:

$$\dot{q}_{\mathrm{Dos}} = f c_{P,\,\mathrm{Dos}} (T_{\mathrm{Dos}} - T_{\mathrm{r}}) \tag{6}$$

where f is the reactant flow rate (mol/s), $c_{P,\,\mathrm{Dos}}$ the specific heat capacity of the dosed liquid (J/mol K) and T_{Dos} (K) is the temperature of the dosed liquid. The crucial heat-flow rate $\dot{q}_{\mathrm{Flow}}$ shown in Figs. 1 and 2 is generally expressed according to the following steady state equation:

$$\dot{q}_{\mathrm{Flow}} = UA(T_{\mathrm{r}} - T_{\mathrm{j}}) \tag{7}$$

where A is the total heat-transfer area (m^2) and U is the overall heat-transfer coefficient (W/m^2 K). U consists of two main coefficients of heat-transfer:

$$\frac{1}{U} = \frac{1}{h_{\mathrm{r}}} + \frac{1}{\varphi} \tag{8}$$

where h_{r} is the reactor-sided steady-state heat-transfer coefficient (W/m^2 K) and ϕ is the device specific heat-transfer coefficient (W/m^2 K). For a standard reaction calorimeter with a cooling jacket (see Fig. 1 left side) it can be further expressed as follows:

$$\frac{1}{\varphi} = \frac{L}{\lambda_W} + \frac{1}{h_{\mathrm{j}}} \tag{9}$$

where h_{j} is the jacket-sided steady-state heat-transfer coefficient (W/m^2 K) respectively, λ_{W} the heat conductivity of the reactor wall (W/m K), and L is the thickness of the reactor wall (m). If the reactor wall contains a Peltier element, a more sophisticated description for the device specific heat-transfer is required (compare to Eq. (17)). But the following discussion is still valid.

The two steady-state heat-transfer coefficients h_{r} and h_{j} could be further described by physical properties of the system. The reactor-sided heat-transfer coefficient h_{r} in Eq. (8), is strongly dependent on the physical properties (heat capacity, density, viscosity, and thermal conductivity) as well as on the fluid dynamics inside the reactor. Similarly the jacket-sided heat-transfer coefficient h_{j} depends on the properties and on the fluid dynamics of the chosen cooling liquid [33]. Thus, U generally varies during the measurement of a chemical reaction because of mainly two reasons:

1. h_{r} varies because the physical properties of the reaction mixture change during a reaction (e.g. viscosity increase during a polymerization reaction);
2. depending on the calorimetric system chosen, h_{j} may vary because the jacket temperature T_{j} varies during the measurement of a reaction and consequently the physical properties of the cooling liquid that determine h_{j}. This does only apply for reaction calorimeters with a cooling jacket (see Fig. 1, left side).

Not only U but also the heat-transfer area A in Eq. (8) can change during a reaction measurement because of volume changes caused by density changes or dosing of reactants. For a Peltier calorimeter designed according to Fig. 1 A does not change.

As mentioned Eq. (8) is only valid at steady-state conditions, when the heat-flow rate through the reactor wall is constant. However, if a reaction is taking place, the heat-flow rate through the reactor wall might vary depending on the calorimetric principle applied (see below). Therefore, heat accumulation occurs inside the reactor wall or inside the Peltier element as well as the reactor- and jacket-sided film layers. A heat-flow model for the reactor wall was proposed by Karlsen and Villadsen [34] and Zaldívar et al. [35]. The dynamic heat-transfer in the reaction mixture as well as in

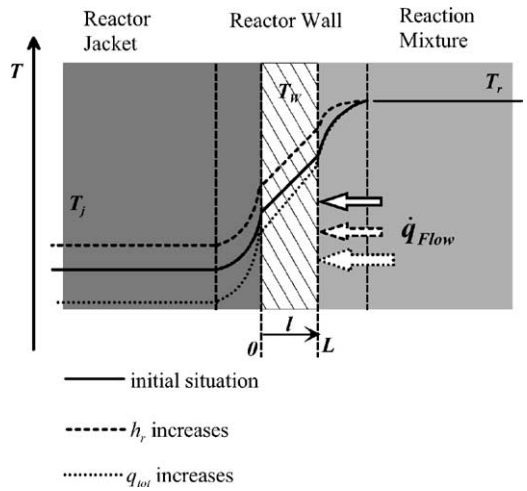

Fig. 3. Steady-state temperature profile in a heat-flow reaction calorimeter when heat flows from the reactor-content ($T = T_r$) through the reactor wall ($T = T_W(l)$) into the jacket ($T = T_j$). The reactor temperature is controlled at isothermal conditions by varying T_j.

the cooling liquid were not considered. Due to the complexity of an exact physical calculation of a dynamically changing $\dot{q}_{Flow}$ it is generally completely neglected and the steady-state Eq. (8) is also used to describe a time-varying calorimetric signal.

2.3.1. Steady-state isothermal heat-flow balance of a heat-flow reaction calorimeter

Fig. 3 shows the steady-state temperature profile through the reactor wall at different operating conditions. The solid line represents the initial situation assuming constant $\dot{q}_{tot}$ and therefore, constant heat-flow rate through the reactor wall ($\dot{q}_{Flow}$). There are basically two different events that will cause a change of this situation:

(1) A change of the reactor-sided heat-transfer, e.g. an increasing h_r. Therefore, the overall heat-transfer coefficient U (Eq. (8)) will increase. The resulting temperature profile is shown by the dashed line. As $\dot{q}_{tot}$ does not change, $\dot{q}_{Flow}$ is not allowed to change as well because T_r is controlled at isothermal conditions. Therefore, the temperature profiles inside the cooling liquid and the reactor wall will only be shifted to another level but do not change their shape (Assuming that h_j and λ_W are independent of temperature). However, as h_r is increased the temperature difference $T_r - T_W(L)$ has to decrease in order to keep $\dot{q}_{Flow}$ constant. Thus, the jacket temperature T_j will have to be increased by the controller in order to keep T_r constant.

(2) A change of the total heat-flow rate $\dot{q}_{tot}$, e.g. an increasing $\dot{q}_{tot}$. The resulting temperature profile is shown by the dotted line. As $\dot{q}_{tot}$ increases, also $\dot{q}_{Flow}$ has to increase because T_r is controlled at isothermal conditions. Assuming that h_r, h_j, and λ_W are independent of the temperature, they remain constant, and thus, the jacket temperature T_j has to be lowered by the controller in order to keep T_r constant.

According to Fig. 3, the reactor wall as well as the cooling liquid are the main dynamic elements in a heat-flow reaction calorimeter as their temperatures change most during a reaction measurement. The temperature of the cooling liquid T_j was assumed to be homogeneous over the whole reactor jacket except the jacket-sided film layer. This assumption is reasonable as long as the flow of the cooling liquid is fully turbulent. If T_j is not homogeneous, the measured jacket temperature has to be replaced by a mathematically modified jacket temperature [36].

Only the inner heat-flow balance shown in Fig. 2 ($\dot{q}_{Comp} = 0$ W) has to be considered for reaction calorimeters based on the heat-flow principle. The bound of the steady-state heat-flow balance is the outer reactor wall ($l = 0$) including the jacket-sided film layer described by h_j. The steady-state isothermal heat-flow balance can thus, be expressed as follows:

$$\dot{q}_{Stirr} + \dot{q}_{Dos} + \dot{q}_{tot} = \dot{q}_{Flow} + \dot{q}_{Lid} \quad (10)$$

where $\dot{q}_{tot}$ (W) is the total heat-flow rate of the reaction mixture (Eq. (3)). The heat-flow rates $\dot{q}_{Stirr}$ and $\dot{q}_{Dos}$ were already explained in Eqs. (5) and (6). The heat-flow rate through the reactor wall $\dot{q}_{Flow}$ (W) is generally calculated according to the steady-state Eqs. (7) and (8) though the heat-flow through the reactor wall is clearly dynamic. This could lead to errors if $\dot{q}_{tot}$, calculated by Eq. (10), is used to get kinetic informations (see discussion below).

However, the overall heat-transfer coefficient U and the heat-transfer area A in Eq. (8) are usually unknown and can change during the course of a reaction (see above). Conventionally these two parameters have to be calibrated by means of a calibration heater (see Fig. 1) before and after a reaction experiment. Unfortunately such a calibration is not possible during the reaction. Therefore, a change of U or A caused by the chemical reaction will cause an error in the determined $\dot{q}_{tot}$.

The remaining heat-flow rate in Eq. (10) is $\dot{q}_{Lid}$ the heat losses through the reactor lid. It is strongly dependent on the convection conditions inside the reactor and on the temperature of the reactor lid. For example, $\dot{q}_{Lid}$ could be expressed as follows:

$$\dot{q}_{Lid} = k_{Lid}(T_r - T_{Amb}) \quad (11)$$

where k_{Lid} is an empiric proportional coefficient (W/K) depending on the reaction conditions and T_{Amb} is the ambient temperature (K). Alternatively, $\dot{q}_{Lid}$ could also be described as a function of the vapor pressure of the reactor-content.

2.3.2. Steady-state isothermal heat-flow balance of a power-compensation reaction calorimeter

Fig. 4 shows the steady-state temperature profile from the compensation heater through the reactor-content and wall into the cooling liquid at different operating conditions. The

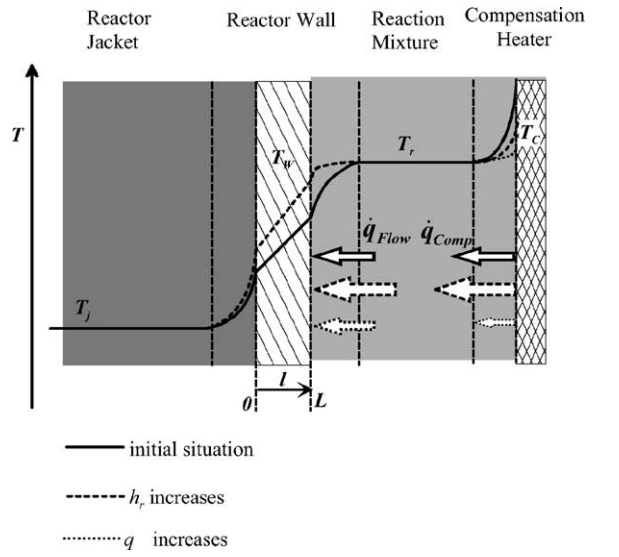

Fig. 4. Steady-state temperature profile in a power-compensation calorimeter when heat flows from the compensation heater ($T = T_C$) into the reactor ($T = T_r$) and from the reactor through the reactor wall ($T = T_W(l)$) into the jacket ($T = T_j$), controlled isothermally by an external cryostat). The reactor temperature is controlled at isothermal conditions by varying the power of the compensation heater ($\dot{q}_{Comp}$).

solid line represents the initial situation assuming no heat release or uptake ($\dot{q}_{tot} = 0$), and therefore, constant heat-flow through the reactor wall ($\dot{q}_{Flow}$) and constant power of the compensation heater $\dot{q}_{Comp}$. There are basically two different events that will cause a change of this situation. Only deviations to the analogous discussion of Fig. 3 will be mentioned here:

(1) A change of the reactor-sided heat-transfer, e.g. an increasing h_r. The resulting temperature profile is shown by the dashed line in Fig. 4. In contrast to Fig. 3, $\dot{q}_{Flow}$ increases as T_j and T_r are controlled at isothermal conditions. In order to keep T_r at isothermal conditions the power of the compensation heater ($\dot{q}_{Comp}$) has to be increased by the controller. Assuming identical heat-transfer conditions on the heater wall as on the reactor wall, the heat-transfer coefficient on the heater surface will increase as well. Thus the temperature of the compensation heater (T_C) might decrease, as indicated in Fig. 4, however, this depends on the situation. It is also possible that the heat-transfer coefficient on the heater surface is larger than h_r on the reactor wall if the compensation heater is placed close to the stirrer.
(2) A change of the total heat-flow rate, e.g. an increasing $\dot{q}_{tot}$. The resulting temperature profile is shown by the dotted line. In contrast to Fig. 3 $\dot{q}_{Flow}$ and the temperature profile through the reactor wall remain constant as T_r and T_j are controlled isothermally. In order to keep T_r constant, the power released by the compensation heater ($\dot{q}_{Comp}$) is decreased resulting in a lower T_C.

According to Fig. 4 the compensation heater is the main dynamic element of a power-compensation reaction calorimeter as its temperature changes during a reaction measurement. The reactor wall has to be considered as a secondary dynamic element if $\dot{q}_{Flow}$ changes during a reaction. Similar to the heat-flow principle only the inner heat-flow balance shown in Fig. 2 has to be considered for this type of calorimeter. The boundary of the steady-state heat-flow balance is the inner reactor wall ($l = L$). The steady-state isothermal heat-flow balance can thus be expressed as follows:

$$\dot{q}_{Stirr} + \dot{q}_{Dos} + \dot{q}_{tot} + \dot{q}_{Comp} = \dot{q}_{Flow} + \dot{q}_{Lid} \quad (12)$$

The description of the different heat-flow rates was already given above. The only new term in Eq. (12) is the power of the compensation heater $\dot{q}_{Comp}$:

$$\dot{q}_{Comp} = U_{Comp} I_{Comp} \quad (13)$$

where U_{Comp} is the voltage (V) and I_{Comp} is the current (A) of the compensation heater. As the heat released by the compensation heater is directly measured in terms of electrical power, changes of the heat-transfer coefficient on the compensation heater do not affect the steady-state heat-flow balance.

For a reaction, in which the heat-flow rate through the reactor wall $\dot{q}_{Flow}$ remains constant during the whole time period (constant base-line), $\dot{q}_{Flow}$ does not have to be calculated explicitly. However, it should be noted that the overall heat-transfer coefficient U or the heat-transfer area A (see Eq. (7)) generally change during the course of a reaction, and thus, $\dot{q}_{Flow}$ will change. This will cause a base-line change in the determined $\dot{q}_{tot}$. The dynamics of the heat-transfer through the reactor wall as well as the compensation heater is generally neglected but could lead to an additional error in the determined $\dot{q}_{tot}$ especially if it is used to calculate kinetic informations (see discussion below).

2.3.3. Steady-state isothermal heat-flow balance of a heat-balance reaction calorimeter

Fig. 5 shows the steady-state temperature profile through the reactor wall as well as the jacket wall at different operating conditions analogous to the discussion of the heat-flow calorimeter. The temperature profiles shown in Fig. 5 are identical to the temperature profiles shown in Fig. 3. Therefore, the comments to Fig. 3 are also valid for the heat-balance calorimeter. Additionally the ambient as well as the jacket wall temperatures were considered. The heat-flow caused by the temperature difference between the cooling liquid T_j and the T_{Amb} is slightly changing for the three different situations shown in Fig. 5. The amount of this change depends strongly on the quality of the thermal insulation around the jacket wall.

According to Fig. 5, in a heat-balance calorimeter the reactor wall, the jacket wall as well as the cooling liquid are the main dynamic elements, as they change their temperatures during a reaction measurement. The temperature of the cooling liquid T_j cannot be assumed to be homogeneous over the whole jacket as the flow rate of the cooling liquid

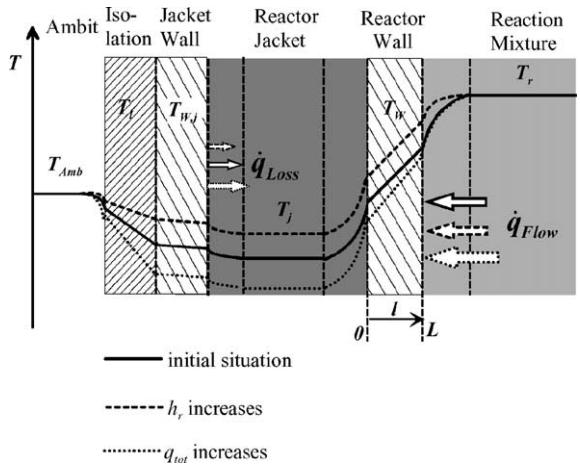

Fig. 5. Steady-state temperature profile in a heat-balance calorimeter when heat flows ($\dot{q}_{\mathrm{Flow}}$) from the reactor-content ($T = T_{\mathrm{r}}$) through the reactor wall ($T = T_{\mathrm{W}}(l)$) into the jacket ($T = T_{\mathrm{j}}$). The reactor temperature is controlled at isothermal conditions by varying T_{j}. An additional heat-flow rate ($\dot{q}_{\mathrm{Loss}}$) from the ambit through the thermal insulation ($T = T_{\mathrm{l}}$) and the jacket wall ($T = T_{\mathrm{W,j}}$) into the cooling liquid is shown.

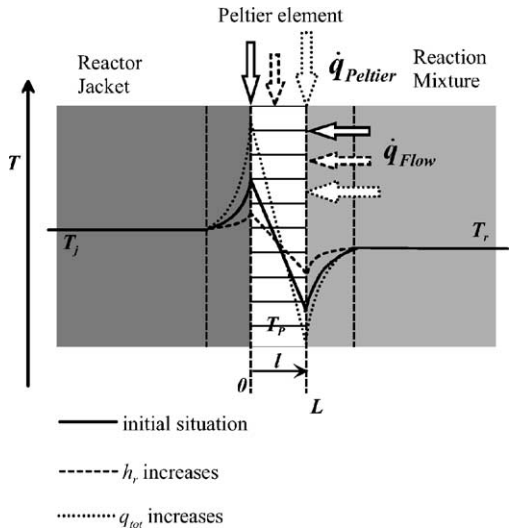

Fig. 6. Steady-state temperature profile in a Peltier calorimeter when heat flows ($\dot{q}_{\mathrm{Flow}}$) from the reactor-content ($T = T_{\mathrm{r}}$) through the Peltier element ($T = T_{\mathrm{P}}(l)$) into the jacket ($T = T_{\mathrm{j}}$), controlled isothermally by an external thermostat). The reactor temperature is controlled at isothermal conditions by varying the power of the Peltier element ($\dot{q}_{\mathrm{Peltier}}$).

has to be chosen low enough in order to be able to measure a temperature difference between inlet $T_{\mathrm{j,\,IN}}$ and outlet temperature $T_{\mathrm{j,\,OUT}}$ of the cooling liquid (see Fig. 2). Therefore, the temperature of the cooling liquid T_{j}, used in the following calculations, should be corrected on the basis of $T_{\mathrm{j,\,IN}}$ and $T_{\mathrm{j,\,OUT}}$ (e.g. [6,36]).

For the heat-flow as well as the power-compensation calorimeter only the inner heat-flow balance in Fig. 2 was considered. For the heat-balance calorimeter ($\dot{q}_{\mathrm{Comp}} = 0\,\mathrm{W}$) both, the inner and the outer heat-flow balance, have to be taken into account. It should be noted that the outer heat-flow balance indicated in Fig. 2 also contains the reactor cover. Depending on the calorimetric system the situation can differ from this ideal picture and thus part of the heat losses through the reactor cover will not be assessed by the outer heat-flow balance. However, for the simplification ideal behavior is assumed and therefore the steady-state isothermal heat-flow balance can be expressed as follows:

$$\dot{q}_{\mathrm{Stirr}} + \dot{q}_{\mathrm{Dos}} + \dot{q}_{\mathrm{tot}} = \dot{q}_{\mathrm{Loss}} + \dot{q}^{\mathrm{OUT}}_{\mathrm{Fluid}} - \dot{q}^{\mathrm{IN}}_{\mathrm{Fluid}} \quad (14)$$

The description of some of the different heat-flow rates was already given above. In Eq. (14), a new heat loss term $\dot{q}_{\mathrm{Loss}}$, is introduced. It describes all heat losses from the outer reactor wall to the environment. Similar to Eq. (11), a general equation can be chosen to describe $\dot{q}_{\mathrm{Loss}}$:

$$\dot{q}_{\mathrm{Loss}} = k_{\mathrm{Loss}}(T_{\mathrm{j}} - T_{\mathrm{Amb}}) \quad (15)$$

where k_{Loss} is an empiric proportional coefficient (W/K) and T_{Amb} the ambient temperature (K). In contrast to k_{Lid}, k_{Loss} does not depend on the conditions inside the reactor and should, therefore, be easier to calibrate. The other two new heat-flow rates in Eq. (14) are the heat pumped by the cooling liquid, $\dot{q}^{\mathrm{IN}}_{\mathrm{Fluid}}$ and $\dot{q}^{\mathrm{OUT}}_{\mathrm{Fluid}}$:

$$\dot{q}^{\mathrm{OUT}}_{\mathrm{Fluid}} - \dot{q}^{\mathrm{IN}}_{\mathrm{Fluid}} = \dot{m} c_{P,\,\mathrm{Fluid}}(T_{\mathrm{j,\,OUT}} - T_{\mathrm{j,\,IN}}) \quad (16)$$

where $\dot{m}$ is the mass flow of the cooling liquid (kg/s) and $c_{P,\,\mathrm{Fluid}}$ its heat capacity (J/kg/K). By Eq. (16) the dynamics of the cooling liquid is taken into account. It is important to note that the problematic term $\dot{q}_{\mathrm{Flow}}$, present in the heat-flow balances of the power-compensation and the heat-flow calorimeters, could be eliminated by considering an outer heat-flow balance. But as shown above, the heat-transfer through the reactor wall as well as the temperature of the jacket wall are clearly dynamic. This could lead to errors if $\dot{q}_{\mathrm{tot}}$, calculated by Eq. (14), is used to get kinetic informations (see discussion below).

2.3.4. Steady-state isothermal heat-flow balance of a Peltier reaction calorimeter

Fig. 6 shows the steady-state temperature profile from the reactor content through the Peltier element into the cooling liquid at different operating conditions. The solid line represents the initial situation assuming, e.g. $h_{\mathrm{r}} = h_{\mathrm{j}}$, constant total heat-flow rate $\dot{q}_{\mathrm{tot}}$ and therefore, constant heat-flow rate through the reactor-sided plate of the Peltier element ($\dot{q}_{\mathrm{Flow}}$). There are basically two different events that will cause a change of this situation. Only deviations to the analogous discussion of Fig. 3 will be mentioned here:

(1) A change of the reactor-sided heat-transfer, e.g. an increasing h_{r}. The resulting temperature profile is shown by the dashed line. As h_{r} increases the temperature difference $T_{\mathrm{r}} - T_{\mathrm{P}}(L)$ has to decrease in order to keep $\dot{q}_{\mathrm{Flow}}$ constant. Thus, the temperature difference over the Peltier element as well as their power consumption ($\dot{q}_{\mathrm{Peltier}}$) will decrease. Consequently less heat has to be removed by the cooling liquid resulting in a smaller temperature difference $T_{\mathrm{P}}(0) - T_{\mathrm{j}}$.

(2) A change of the total heat-flow rate $\dot{q}_{tot}$, e.g. an increasing $\dot{q}_{tot}$. The resulting temperature profile is shown by the dotted line. As h_r remains constant and $\dot{q}_{Flow}$ increases the temperature difference $T_r - T_P(L)$ increases. Consequently the temperature difference over the Peltier elements increases and additionally more heat has to be removed. Therefore, $\dot{q}_{Peltier}$ increases and a larger heat-flow has to be removed by the cooling liquid, resulting in a larger temperature difference $T_P(0) - T_j$ (assuming that h_j is independent of the temperature).

According to Fig. 6 the Peltier element is the main dynamic element, as it changes its temperature during a reaction measurement. Fig. 2 can be applied to a Peltier calorimeter according to Fig. 1 ($\dot{q}_{Comp} = 0\,W$, $\dot{q}_{Flow}$ only through the bottom of the reactor wall and the heat-flow rate $\dot{q}_{Peltier}$ has to be introduced). Similar to a heat-flow or power-compensation calorimeter only the inner heat-flow balance in Fig. 2 has to be considered. The boundary of the steady-state heat-flow balance is the centerline of the Peltier element ($l = 1/2\,L$). The steady-state isothermal heat-flow balance can thus, be expressed by Eq. (10). However, the problematic term $\dot{q}_{Flow}$ can now be expressed based on the measured current and temperature difference of the Peltier element (not equal to $\dot{q}_{Peltier}$, e.g. [5]):

$$\dot{q}_{Flow} = -S\,I_{Pelt}\,T_P(L) - \tfrac{1}{2}R\,I_{Pelt}^2 + \kappa(T_P(L) - T_P(0)) \quad (17)$$

where S is the Seebeck coefficient (V/K), I_{Pelt} (A) the current through the Peltier element (cooling current is negative), R the electrical resistance of the Peltier elements (Ω) and κ is the absolute heat conductivity through the Peltier element (W/K). The device specific Peltier parameters (S, R, and κ) have to be calibrated in advance. It is important to note that the problematic term $\dot{q}_{Flow}$, present in the heat-flow balances of the power-compensation and the heat-flow calorimeters, for the Peltier calorimeter was eliminated by the steady-state approximation given in Eq. (17). But as shown above, the heat-transfer through the Peltier element is clearly dynamic. This could lead to errors if $\dot{q}_{tot}$, calculated by Eqs. (10) and (17), is used to get kinetic informations (see discussion below). Therefore, Nilsson et al. [29] introduced heat accumulation terms in the calculation of $\dot{q}_{tot}$.

2.4. Dynamics of an isothermal reaction calorimeter

If calorimetry is not only used to determine the total amount of heat released or absorbed by a certain process, but also to provide information about the time profile of the total heat-flow rate the dynamics of the measurement system and possible correction methods should be considered [3,4,8,29,34,37,38].

If $\dot{q}_{tot}$ is still calculated based on a steady-state isothermal heat-flow balance the following error sources might cause deviations from ideal behavior and consequently a time distortion of $\dot{q}_{tot}$:

2.4.1. Source A: Deviations from isothermal controlling

If the total time constant of the apparatus is similar or even larger than the time constants of the chemical reactions investigated, the control circuit of the reaction calorimeter will no more be able to control the reaction temperature at isothermal conditions. Consequently heat accumulation will take place in the reactor-content and should be considered in the heat-flow balances.

2.4.2. Source B: Dynamic elements

Depending on the calorimetric principle applied, the constant temperature is maintained by different dynamic elements (reactor wall, compensation heater, Peltier element or cooling liquid). In order to maintain an isothermal reactor temperature they will have to change their temperature (see Figs. 3–6) and therefore, heat accumulation inside of these elements will occur.

2.4.3. Source C: Time constants of temperature sensors

Temperature sensors have their own time constant. Additionally the heat conduction path from the site of the event to the measuring sensor can increase the observed time constant.

2.5. Assessment of the four basic reaction calorimetric principles for isothermal measurements

2.5.1. Heat-flow

As in a heat-flow calorimeter the measured signal is the temperature difference between reactor-content and reactor jacket, the flow rate of the cooling liquid can be chosen to be high without decreasing the quality of the signal. However, the heat-transfer through the reactor wall has to be calibrated with a calibration heater and changes during a reaction cannot be handled correctly in this standard setup.

2.5.2. Power-compensation

From the technical point of view the power-compensation technique is the simplest technique to implement because the temperature of the cooling liquid T_j remains constant. Another advantage of this technique is the direct measurement of the electrical power required to maintain the temperature T_r at a constant level. The main drawbacks of this technique are the possible hot spots on the surface of the compensation heater. It is therefore crucial to check the ratio of reactor volume to heat-transfer surface of the system and to place the compensation heater optimally in the flow field of the stirrer. Another big drawback of this technique is that the constant heat-flow through the reactor wall makes the measured signal more sensitive to a changing heat-transfer (change of U or A in Eq. (7)) than a heat-flow calorimeter [15,21]. If no corrections for a changing heat-transfer through the reactor wall during a reaction

are made, the determined total heat-flow rate ($\dot{q}_{tot}$) will be incorrect.

2.5.3. Heat-balance

The main advantage of this technique is that the determined signal $\dot{q}_{tot}$ is independent of changes of the heat-transfer through the reactor wall during a reaction experiment. In contrast to all other techniques an additional calibration heater must be introduced if informations about the heat-transfer on the reactor wall are also required, e.g. for later scale-up. The flow rate of the cooling liquid must meet two requirements that are difficult to accomplish simultaneously. On the one hand, the flow rate of the circulating fluid must be high enough to realize a fast heat-transfer into the jacket in order to control the reaction temperature at a constant level. On the other hand, it should be low, to establish a temperature difference over the jacket large enough to be measured accurately. The influence of the ambient temperature on the finally determined $\dot{q}_{tot}$ signal is large compared to all other principles. Therefore, good isolation of the reactor jacket is required.

2.5.4. Peltier

The main advantage of this technique is that the determined signal $\dot{q}_{tot}$ is independent of changes of the heat-transfer through the reactor wall during a reaction experiment. A drawback of this technique is that the Peltier elements must be pre-calibrated.

2.5.5. Dynamics of the four calorimeters

Apart from the general aspects discussed above, the dynamics of the four different principles differ significantly:

2.5.5.1. Deviations from isothermal controlling. A common feature for the heat-flow and especially heat-balance calorimeters is the fairly slow control of the jacket temperature [39] because the main dynamic element is the reactor wall and the cooling liquid. Therefore, even though the calorimeters are run in isothermal mode, heat accumulation in the reactor content has to be considered because the reaction temperature still varies in the range of some degrees Celsius [5]. The thermostatic units used to vary the temperature of the cooling liquid have to be fast and powerful [12]. Power-compensation calorimeters, however, can be tuned to control T_r very precisely even for fast and strongly exothermal reactions [3,40]. Peltier calorimeters show a dynamic behavior in between the other two.

2.5.5.2. Dynamic elements. As shown above heat-flow and heat-balance calorimeters have two common dynamic elements: the reactor wall as well as the cooling liquid. As the flow rates of the cooling liquid are generally higher for a heat-flow calorimeter than for a heat-balance calorimeter the temperature changes, and thus the disturbance by the dynamic element, will be larger for the heat-balance calorimeter.

In power-compensation calorimeters, the reactor wall is a dynamic element similar to the heat-flow and heat-balance calorimeters. However, as shown in Fig. 4 its temperature changes during a reaction measurement are generally much smaller compared to all other principles. Further, it should be considered that in a heat-flow or heat-balance calorimeter h_j will generally vary as a function of T_j leading to even larger temperature changes of the reactor wall. The main dynamic element in a power-compensation calorimeter is therefore, the compensation heater. But the heat accumulation inside the heater element is generally much smaller compared to the heat accumulated in the wall of a Peltier or even heat-flow or heat-balance calorimeter.

In a Peltier calorimeter, the main dynamic element is the Peltier element. As Peltier elements cannot be used in direct contact with the cooling liquid or the reaction mixture they are generally introduced between two covering plates. This construction will lead to a rather slow behavior compared to a power-compensation calorimeter, however comparable to a heat-flow or heat-balance calorimeter. Additionally, Eq. (17) to calculate $\dot{q}_{Flow}$ is only valid for steady-state conditions. Therefore, corrections such as heat accumulation must be considered for a reaction measurement [3,29].

Considering the different control principles and dynamic elements, it becomes clear that $\dot{q}_{tot}$ determined by Eqs. (10), (12), (14), and (17) will be less time distorted for a well designed power-compensation calorimeter compared to a Peltier, heat-flow or even heat-balance calorimeter. The power-compensation technique is therefore, the method of choice if fast and strongly exothermal reactions have to be measured under isothermal conditions [3,40].

2.6. Further developments and combinations of the four basic principles

2.6.1. Combination of the heat-flow and heat-balance principle

Most of the commercial available heat-balance calorimeters can be used as heat-flow calorimeters as well [13,26,41] because only little changes on the setup have to be made. However, as mentioned above an optimal flow rate of the cooling liquid inside the reactor jacket might be difficult to achieve in certain applications.

2.6.2. Improvements of the power-compensation technique

Most of these calorimeters aim at combining the power-compensation technique with an additional outer heat-flow balance in order to correct the measured reaction heat-flow rate for changes of the heat-transfer through the reactor wall. Litz [42] introduced an additional intermediate thermostat between the reactor and the outside cooling liquid. The intermediate thermostat is constructed similar to the power-compensation principle and allows an online measurement of the heat-flow through the reactor wall. This principle was the basis for the new design by Zogg et al. [3,40] described below. Schlegel et al. [43] combined

the power-compensation technique with a heat-balance calorimeter in order to improve the dynamics of the temperature control system and to measure the changing heat-transfer coefficient. In the Simular calorimeter from HEL [15] the power-compensation technique can be implemented optionally and is supported with a "pseudo" heat-balance measurement, the CMC approach: the changing baseline of the power-compensation signal is corrected proportional to the measured temperature difference between the inlet and the outlet temperature of the cooling liquid. Schildknecht [20,44] designed a power-compensation calorimeter that uses the reactor wall as heater surface, and therefore, minimizes eventual hot spots on the surface of the heater.

2.6.3. Improvements of the heat-flow principle

Tietze et al. [45] addressed the problem of the changing heat-transfer coefficient in a heat-flow calorimeter and proposed an online measurement based on an oscillation of the temperature of the cooling liquid. BenAmor et al. [46] presented an algorithm for the online detection of the heat-transfer coefficient based on mathematical modeling.

2.6.4. Combination of the power-compensation and Peltier principle

Zogg et al. [3,40] presented a combination of the Peltier and the power-compensation principle. The fast power-compensation principle is applied to control the reaction temperature. Eventual changes of the heat-transfer through the reactor wall ($\dot{q}_{\mathrm{Flow}}$, rather slow processes involved as compared to the changes of $\dot{q}_{\mathrm{React}}$) are measured online by an intermediate thermostat using the Peltier principle (comparable to the design of Litz [42], see above). This concept was patented [47].

2.6.5. Isoperibol calorimeters

For weakly exo- or endothermal reactions the temperature change of T_{r} in an isoperibole reaction calorimeter is rather small, comparable to an isothermal reaction calorimeter. Moritz and co-workers [48,49] presented an isoperibol reaction calorimeter that is inserted into a compensation heater controlled heat-flow device. A changing heat-transfer coefficient during a reaction measurement does not influence the calculated reaction heat-flow rate.

A completely new design for an isoperibol reaction calorimeter was presented by Setaram [50]. According to the differential measurement principle common for thermo-analytical devices such as DSC or DTA, two reaction vessels are run in parallel. One is filled with the reaction components and the other one, e.g. with the solvent. The basic signal used for the evaluation is the temperature difference of the two reactor-contents [51].

2.7. Comparison of available calorimeters

In the following, some of the calorimeters explained above are compared according to three important properties:

2.7.1. Relative detection limit (W/l) (Fig. 7)

The absolute detection limit (W) specifies the smallest heat-flow rate that can still be measured by the calorimeter. The smaller the detection limit the better the calorimeter. Smaller heat-flow rates can no more be distinguished from the noise of the measurement system. The intensity of the measurement noise is generally only related to the physical properties of the measuring system and independent of the sample volume. In contrast the intensity of the measured heat-flow rate is proportional to the sample volume. The absolute detection limit can thus, be decreased by simply increasing the sample volume. Therefore, the detection limit relative to the sample volume (W/l) is shown in Fig. 7 in order to allow a comparison between different calorimeter techniques.

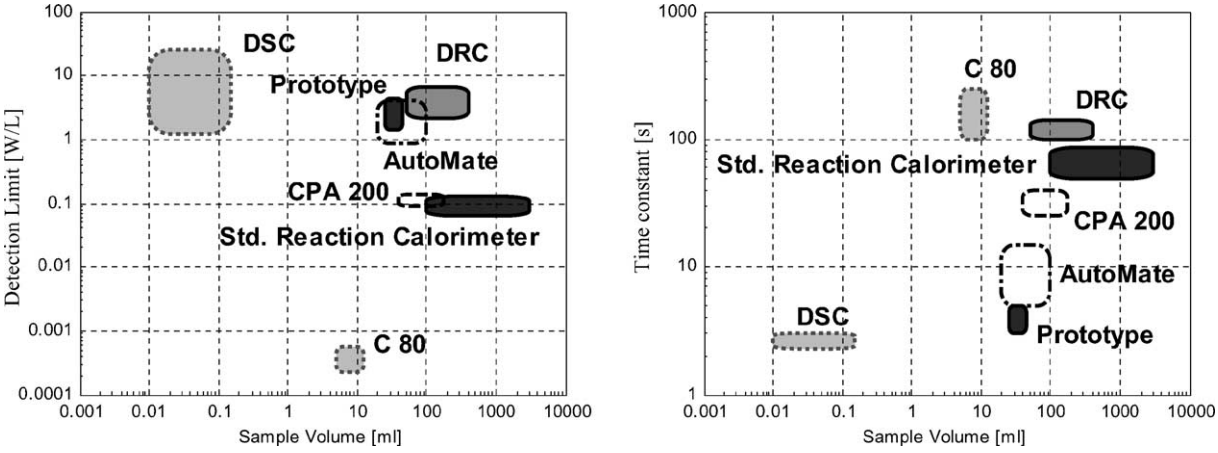

Fig. 7. Comparison of different available reaction calorimeters based on their relative detection limit (W/l) (left side) and their time constant (s) (right side). See text for explanation of the different calorimeters.

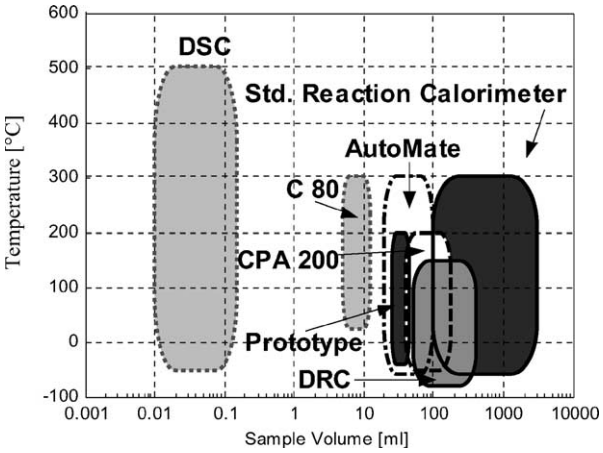

Fig. 8. Comparison of different available reaction calorimeters based on their temperature range (°C). See text for explanation of the different calorimeters.

2.7.2. The time constant (s) (Fig. 7)

The time constant characterizes the inertia of the whole measurement device. It is generally determined by applying a known heat-flow impulse from an external source. As long as the time constant of the calorimeter is smaller than the time constant of the measured process (e.g. chemical reaction) the determined heat-flow rate shows no time distortion. Thus, the smaller the time constant the better the calorimeter.

2.7.3. Temperature range (°C) (Fig. 8)

A third important property of a reaction calorimeter is the temperature range that can be used for reaction measurements.

The values shown in Figs. 7 and 8 are based on manufacturer specifications obtained on request, published example applications as well as user experiences [52]. The following devices are compared:

- *Standard reaction calorimeters*: The standard reaction calorimeters such as the RC1 from Mettler Toledo [11,12], SysCalo from Systag [13], as well as the Simular from HEL [14,15] are shown as a single group (average value).
- *CPA* 200: Medium scale Peltier calorimeter from Chemisens [25].
- *AutoMate*: Small scale power-compensation reaction calorimeter from HEL [14] as well as [23].
- *Prototype*: Small scale power-compensation reaction calorimeter with online baseline correction presented by Zogg et al. [3,40].
- *DRC*: Differential reaction calorimeter from Setaram [50,51].
- In order to allow a comparison to other relevant thermoanalytical measurement devices a standard differential scanning calorimeter device [52] as well as the C80 (differential Calvet-type calorimeter) from Setaram [50] are shown as well.

3. Part 2. Evaluation methods for isothermal calorimetric reaction data

The task of any reaction calorimeter is to determine the total heat-flow rate during a reaction experiment $\dot{q}_{tot}$ (W). In the following a review on different evaluation methods for isothermally measured $\dot{q}_{tot}$ shall be given. The aim of all methods described is to determine the reaction enthalpy and the kinetic model parameters (such as rate constants, reaction orders) of an investigated reaction. If the temperature dependency of the reaction hast to be studied, several isothermal measurements at different temperatures have to be carried out. The results of the individual evaluations can then be plotted, e.g. in an Arrhenius plot in order to calculate the activation energy or to check whether the reaction mechanism did change between the different temperatures. Some of the proposed techniques also allow a simultaneous evaluation of several isothermal measurements at different temperatures by replacing the rate constants by the following Arrhenius approximation:

$$k = k(T_{ref})\mathrm{e}^{-E_A/R(1/T_r - 1/T_{ref})} \quad (18)$$

where T_{ref} is the reference temperature (K), E_A the Arrhenius activation energy (J/mol), and R is the ideal gas constant (J/mol/K).

As indicated in Eq. (3), $\dot{q}_{tot}$ is generally not equal to the reaction heat-flow rate $\dot{q}_{React}$ (Eq. (4)) but is also influenced by any other physical or chemical process where heat is released or absorbed like mixing or phase changes. Care should thus be taken when reaction calorimetric experiments are evaluated for kinetic or safety studies.

Even for a simple reaction example, such as the hydrolysis of acetic anhydride, a significant heat of mixing occurs and should be considered [40,53,54].

Additionally, it should always be kept in mind that the $\dot{q}_{tot}$ determined by a reaction calorimeter also contains measurement errors such as base line drifts, time distortion (compare to the discussion of the dynamic elements in a reaction calorimeter), or ambient temperature influences (Eqs. (11) and (15)).

3.1. Evaluations not requiring a reaction model

3.1.1. Method 0: Determination of the reaction enthalpy by integration of $\dot{q}_{tot}$

The simplest of the model-free evaluation technique that still leads to a physically meaningful result: The integration of the determined $\dot{q}_{tot}$ signal:

$$Q_{tot} = \int_{t=0}^{t=t_f} \dot{q}_{tot}\,\mathrm{d}t = \sum_{i=1\ldots N_R} (-\Delta_r H_i)n_i + Q_{mix} + Q_{Phase} + Q_{Error} \quad (19)$$

where t_f is the integration limit in time (s), Q_{tot} the integral of the total heat-flow rate (J), n_i the number of moles of the

*i*th reaction component (mol), Q_{mix} the heat of mixing (J), Q_{Phase} the heat released or absorbed by phase change processes, and Q_{Error} the sum of all measurement errors (J). It should be noted that the appropriate selection of the integration time limit has a significant influence on the calculated Q_{tot} [55].

For a further evaluation of Q_{tot} the following assumptions are generally made: Q_{mix}, Q_{Phase}, and Q_{Error} are assumed to be negligible, meaning that $\dot{q}_{tot} = \dot{q}_{React}$, and the reaction is assumed to perform in one single rate determining step. If these assumptions are fulfilled, the reaction enthalpy $\Delta_r H$ can thus be calculated directly by the following equation:

$$-\Delta_r H \approx -\Delta H = \frac{Q_{tot}}{n} \tag{20}$$

where ΔH is the total enthalpy change (J/mol). However, in real applications Q_{mix}, Q_{phase}, and Q_{Error} are generally not zero and will therefore be fully integrated into the reaction enthalpy. Once the reaction enthalpy is determined, it is possible to calculate the thermal conversion or fractional heat evolution of the reaction:

$$X_{thermal}(t) = \frac{\int_{\tau=0}^{\tau=t} \dot{q}_{tot}\, d\tau}{Q_{tot}} \tag{21}$$

This thermal conversion can be compared to the chemical conversion of the investigated reaction as long as the assumptions mentioned above are fulfilled or the correspondence between chemical and thermal conversion was verified by another analytical technique [56,57].

If the assumptions made above are not fulfilled and/or informations about the rate constants of the investigated reactions are required, model-based approaches have to be chosen.

3.2. Model-based evaluation methods for single step nth order batch reactions

Most of the model-based evaluations of the calorimetric signal are based on the assumption that the reaction performs in one single step of *n*th order with only one rate determining component concentration. The reactions must be carried out in batch mode (V_r = constant) in order to simplify the evaluation. The general reaction model can therefore be written as follows:

$$\begin{aligned} &A + \ldots \rightarrow \text{Prod} \quad r_A(t) = -kC_A(t)^n \\ &\dot{q}_{React}(t) = \Delta_r H r_A(t) V_r \end{aligned} \tag{22}$$

where C_A is the concentration (mol/m^3) of the rate-determining component A, k, the nth order rate constant [(m^3/mol)$^{n-1}$/s], n the order of the reaction, and r_A is the rate of reaction of component A (mol/m^3/s) (negative sign). As already mentioned earlier, in the field of reaction calorimetry $\dot{q}_{React}$ is generally defined positive for an exothermal reaction (with a negative $\Delta_r H$). The task of the evaluation is to calculate the kinetic parameters k and possibly n. Some methods also determine the thermodynamic parameter $\Delta_r H$ based on this reaction model.

3.2.1. Method I.A: Determination of the kinetic parameters based on the reaction enthalpy determined by prior integration of $\dot{q}_{tot}$

Assuming that Q_{mix}, Q_{Phase}, and Q_{Error} in Eq. (19) are negligible $\Delta_r H$ as well as the thermal conversion can be calculated according to Eqs. (19)–(21). The rate of reaction r_A can then be expressed as follows:

$$r_A(t) = \frac{\dot{q}_{tot}(t)}{V_r \Delta_r H} = -kC_{A,0}^n (1 - X_{thermal}(t))^n \tag{23}$$

where $C_{A,0}$ is the initial concentration of component A. By plotting $\log(r_A)$ versus $\log(1 - X_{thermal})$ it can be verified whether a straight line is obtained. The reaction order n can then be determined from the slope of the line and the rate constant k from the intersection [8,58].

If the reaction order n of component A is known in advance, the reaction model (Eq. (22)) can be integrated. Assuming, e.g. a first order reaction in component A ($n = 1$), the rate constant k can then be determined by the following non-linear least-squares optimization [51,55,59–61]:

$$\min_k \sum_{i=1}^{N_t} \left[X_{thermal}(t_i) - (1 - e^{-kt_i}) \right]^2 \tag{24}$$

where t_i is the ith point in time of the calorimetric measurement and N_t the total number of samples.

3.2.2. Method I.B: Separate determination of the rate constant k as well as the reaction enthalpy $\Delta_r H$ based on the reaction model

For first order reactions ($n = 1$ in Eq. (22)) the reaction model can be integrated and $\dot{q}_{tot}$ can be expressed as follows assuming that $\dot{q}_{tot} = \dot{q}_{React}$:

$$\dot{q}_{tot}(t) = V_r(-\Delta_r H) k C_{A,0} e^{-kt} \tag{25}$$

Therefore, plotting $\log(\dot{q}_{tot})$ versus time should result in a straight line with a slope equal to $-k$. Applications are reported in [31,39,62]. Any reaction period where the assumption $\dot{q}_{tot} = \dot{q}_{React}$ is not fulfilled will be visible in the plot as a deviation from the straight line. Such time periods can then be excluded from the determination of k. An example of such an application is the determination of the rate constant of the hydrolysis of acetic anhydride where a heat of mixing is released during the initial phase [40,54,58,63].

For the same reaction Köhler et al. [63] and Litz [58] determined the reaction enthalpy $\Delta_r H$ from the intercept of the line in the same plot ($\log(\dot{q}_{tot})$ versus time, compare to Eq. (25)). As the heat of mixing only takes place during the initial phase of the reaction, it does not influence the determination of $\Delta_r H$. Walisch and Becker [28,64] described a similar calculation method for the same reaction in order to split the total measured heat Q_{tot} into the heat of mixing Q_{mix} and the enthalpy of reaction $\Delta_r H$. In contrast to Section 3.2.1,

this method represents another way to calculate $\Delta_r H$, alternative to the integration formulated in Eqs. (19) and (20).

3.3. Model-based evaluation methods for more complex reactions

The evaluation Sections 3.2.1 and 3.2.2 can only be applied for single step reactions in batch mode with one single rate-determining component concentration. If the evaluation of the calorimetric signal should be extended to the general case of the semi-batch operation mode ($V_r = V_r(t)$) or to multiple reaction systems including eventual mass-transfer processes, these methods will fail. Therefore, more general evaluation methods were developed.

The basis of these methods is a reaction model represented by a system of ordinary differential equations (compare to Eq. (22)). However, the reaction model can now include more than one chemical reaction as well as mass-transfer or dosing processes. Generally analytical solutions for such reaction models do not exist. Thus, numerical differential equation solvers are used to integrate these models.

The task of the evaluation method is to calculate the unknown parameters of the reaction model. These reaction model parameters (in future indicated as $\theta_{1,\dots,N_P}$) can be rate constants, activation energies, reaction orders, or mass-transfer parameters. Additionally, the reaction enthalpies of the different reaction steps have to be identified as the integration approach formulated by Eqs. (19) and (20) is not feasible any more.

3.3.1. Method II.A: Identification of either the reaction enthalpies or the reaction model parameters $\theta_{1,\dots,N_P}$ if the non-identified counterpart is known

If the reaction enthalpies of each reaction step would be known in advance, the reaction model parameters could be identified by the following non-linear least-squares optimization:

$$\min_{\theta_{1,\dots,N_P}} \sum_{i=1}^{N_t} \left[\dot{q}_{tot}(t_i) - \sum_{j=1}^{N_R} V_r(t_i)(-\Delta_r H_j) r_j(t_i, \theta_{1,\dots,N_P}) \right]^2 \tag{26}$$

where $\theta_{1,\dots,N_P}$ are the unknown reaction model parameters, N_P the number of model parameters, $\Delta_r H_j$ the jth reaction enthalpy (J/mol), N_R the number of reactions, N_t the number of time samples, and r_j is the jth rate of reaction (mol/m^3/s) (positive sign). The rates of reaction are defined by the reaction model. Thus the reaction model has to be integrated for all iterations during the optimization process. This method assumes that $\dot{q}_{tot} = \dot{q}_{React}$. If this assumption is not fulfilled during certain time regions of the measurement (e.g. during the dosing), the corresponding measurement points can be excluded from the summation in Eq. (26).

Examples of this nonlinear parameter identification task, with known reaction enthalpies, are given by Landau et al. [65] who identified three rate constants of a consecutive catalytic hydrogenation, Lunghi et al. [66] who identified the reaction orders and the rate constant of a nitration with BatchCAD [67] and Sbirrazzuoli et al. [68] who identified two rate constants and two reaction orders of a simulated parallel reaction system. All authors repeated the evaluation for several isothermal measurements at different temperatures. In [65,68], the Arrhenius law (Eq. (18)) was directly included into the non-linear optimization (Eq. (26)).

However, the crucial task is to find the appropriate reaction enthalpies. Sbirrazzuoli et al. [68] used pre-defined values for $\Delta_r H_j$ and Lunghi et al. [66] determined a single reaction enthalpy by integration of $\dot{q}_{tot}$ (Eq. (19)). Only the approach of Landau et al. [65], to calculate the reaction enthalpies by a semi-empirical quantum mechanical program [69] could be applied in a general case.

The method can also be applied the other way round: If the parameters $\theta_{1,\dots,N_P}$ would be known in advance, the reaction enthalpies could be calculated according to the following linear least-squares optimization:

$$\min_{\Delta_r H} \sum_{i=1}^{N_t} \left[\dot{q}_{tot}(t_i) - \sum_{j=1}^{N_R} V_r(t_i)(-\Delta_r H_j) r_j(t_i) \right]^2 \tag{27}$$

Zogg et al. [40] initially determined the rate constant of the hydrolysis of acetic anhydride analogous to Section 3.2.2. The reaction enthalpy $\Delta_r H$ was then determined using Eq. (27). The heat of mixing occurring during the dosing period was excluded from the summation in Eq. (27).

3.3.2. Method II.B: Simultaneous identification of the reaction enthalpies and the reaction model parameters

If neither the reaction enthalpies nor the reaction model parameters ($\theta_{1,\dots,N_P}$) can be determined based on external informations or by any of the methods described so far, their determination must be carried out in a single step by the following non-linear least-squares optimization:

$$\min_{\theta_{1,\dots,N_P},\, \Delta_r H_{1,\dots,N_R}} \times \sum_{i=1}^{N_t} \left[\dot{q}_{tot}(t_i) - \sum_{j=1}^{N_R} V_r(t_i)(-\Delta_r H_j) r_j(t_i, \theta_{1,\dots,N_P}) \right]^2 \tag{28}$$

Examples of this non-linear parameter identification are presented by several authors: Evans et al. [70] identified two rate constants, two reaction orders and two reaction enthalpies of a consecutive amination using an in-house program. The evaluation program TA-kin [71], was used in several applications to identify rate constants, reaction enthalpies and activation energies in one step [72–74]. Pastré et al. [22] used the ACSL optimization toolbox [75] to identify the rate constant, reaction enthalpy and reaction orders of a one step semi-batch reaction. Dyer et al. [76] identified three rate constants, two reaction orders and three reaction enthalpies of a consecutive Vilsmeier reaction using an

in-house program. Balland et al. [77] presented a genetic optimization algorithm and identified two rate constants, three reaction orders and two reaction enthalpies of a saponification reaction. The heat of mixing was modeled and identified as well.

Zogg et al. [80,3] identified two reaction enthalpies, two rate constants, two activation energies as well as reaction orders of a two step consecutive reaction. The evaluation however performed much better if additional online measured reaction spectra were included into the evaluation (see below). Commercial calculation packages that are able to carry out such a parameter identification task are BatchCAD [67] BatchReactor [78], and ChemCAD [79].

3.4. Evaluations based on a reaction model and supported by additional analytics

3.4.1. Method III.A: Identification of the reaction model parameters $\theta_{1,\dots,N_P}$ using additional concentration measurements obtained by a calibrated analytical technique

Machado et al. [81] investigated a complex parallel and consecutive reaction system. The enthalpies of reaction were determined in advance and finally two rate constants (including the activation energies) where fitted to the calorimetric data. The nonlinear optimization is similar to the one described by Eq. (26) but additionally to the total heat-flow rate $\dot{q}_{tot}$, concentration measurements were included into the objective function:

$$\min_{\theta_{1,\dots,N_P}} \left\{ \sum_{i=1}^{N_t} W_Q \left[\dot{q}_{tot}(t_i) - \sum_{j=1}^{N_R} V_r(t_i)(-\Delta_r H_j) r_j(t_i, \theta_{1,\dots,N_P}) \right]^2 + \sum_{s=1}^{N_C} \sum_{i=1}^{N_{obs}} W_C \left[c_{measured,\,s}(t_i) - c_{calc,\,s}(t_i, \theta_{1,\dots,N_P}) \right]^2 \right\} \quad (29)$$

where W_Q and W_C are user-defined weighting functions, N_C the number of measured components, N_{obs} the number of concentration observations, $c_{measured,\,s}$ the measured and $c_{calc,\,s}$ the calculated concentration (using the reaction model) of the sth component. The same evaluation principle was applied to a more complex heterogeneous hydrogenation reaction with more than ten model parameters [82]. Because the hydrogen-uptake rate was measured as well, the reaction enthalpies were also determined in an initial step. In both examples, several isothermal experiments were combined to one data set and evaluated at the same time by using Eq. (18).

The combined evaluation of the calorimetric and concentration data is also available in commercial software packages such as BatchCAD [67], ChemCAD [79], or BatchReactor [78]. The application of this combined evaluation approach was also reported by Dyer et al. [76] but no details about the underlying mathematics were given. It should be noted that any kind of concentration measurement carried out by, e.g. HPLC, GC, or spectroscopic techniques, require a time consuming pre calibration of the analytical devices.

3.4.2. Method III.B: Identification of the reaction model parameters $\theta_{1,\dots,N_P}$ using additional measurement of a gas production or uptake rate

The nonlinear optimization described in Eq. (26) (Section 3.3.1) requires the knowledge of the reaction enthalpies. The overall optimization according to Eq. (28) (Section 3.3.2) to estimate thermodynamic and kinetic reaction parameters at the same time might be difficult to solve in certain applications [80]. Therefore, Sempere et al. [83] calculated the reaction enthalpies of the reaction steps during a complex N-oxidation reaction based on the additionally measured oxygen production. All other seven reaction model parameters could then be calculated by Eq. (26). Le Blond et al. [84] calculated the reaction enthalpies of the reaction steps during the hydrogenation of a nitro group based on the additionally measured hydrogen uptake. The rate constants of the reactions involved were then calculated on the basis of infrared measurements and not calorimetric measurements.

3.4.3. Method III.C: Simultaneous identification of the reaction model parameters $\theta_{1,\dots,N_P}$ and the reaction enthalpies using additionally measured and uncalibrated reaction data

As mentioned the general evaluation method II.B might be difficult to handle for certain reaction examples. Therefore, Zogg [3] developed a combined evaluation method that allows the simultaneous evaluation of reaction calorimetric data (according to Eq. (28)) and on-line measured infrared reaction spectra (without calibration). The combination of the calorimetric and infrared objective function was done similar to Eq. (29), the calculation of the weighting factors however, was done automatically. The combined evaluation algorithm was applied to a simple reaction example, the hydrolysis of acetic anhydride [85] and to a consecutive two step reaction example using different possible reaction models [80]. The method was compared to method II.B (see above). The proposed evaluation principle could be applied to any additionally measured reaction data as long as the relationship between the reaction model and the output of the applied analytical sensor is linear. Possible additional information sources could be gas uptake or production rates or uncalibrated GC or HPLC measurements. The combination of calorimetry and infrared spectroscopy nowadays is a common tool to investigate reactions [22,55,84,86–88].

3.5. Assessment of the different evaluation methods

All mentioned evaluation methods are summarized in Table 1. The sensitivity of the methods towards deviations from the common assumption that $\dot{q}_{tot} = \dot{q}_{React}$ (compare to Eqs. (3) and (19)) are judged as follows: high for the model free evaluation and Section 3.2.1 as all possible deviations

Table 1
Overview on the different evaluation methods (O, I.A, I.B, II.A, II.B, III.A, III.B; see text) for the total heat-flow rate $\dot{q}_{tot}$ measured by a reaction calorimeter

		O[a]	I.A	I.B	II.A		II.B	III.A	III.B	III.C
	Equation Nr.	20	23, 24	25	26	27	28	29		
Identified reaction parameters	$\theta_{1,\dots,N_P}$		✓	✓	✓		✓	✓	✓	✓
	$\Delta_r H_j$[b]	✓		✓		✓	✓			✓
Requires integration of $\dot{q}_{tot}$		✓	✓							
Requires external knowledge of	$\theta_{1,\dots,N_P}$					✓				
	$\Delta_r H_j$[b]				✓			✓	✓	
Sensitivity to possible deviations from the assumption $\dot{q}_{tot} = \dot{q}_{React}$		high		medium				low		
exclusion of data points possible where $\dot{q}_{tot} \neq \dot{q}_{React}$				✓	✓	✓	✓	✓	✓	✓
Additional analytical information included								✓[c]	✓[d]	✓[e]
	Calibration required							✓		
Only for *n*th order single step reactions with one rate determining component		✓	✓	✓						
Complexity of identifiable reaction models		–	low		medium			*very*high	high	

[a] Model free evaluation method.
[b] Reaction enthalpies of each reaction step.
[c] Concentration measurements.
[d] Gas production or uptake rate.
[e] Reaction data that is linearly related to the identified reaction model (e.g. infrared reaction spectra).

from the ideally assumed behavior are directly integrated into $\Delta_r H$ and influence also the determined rate constants [3]. Medium for methods I.B and II.B as exclusion of data points, where ideal behavior is not fulfilled, is possible and because the model based evaluation acts like a filter for the estimation of the reaction enthalpies and model parameters. Low for methods III.A, III.B, and III.C because the different analytical signals are included into the evaluation that are not influenced by the same disturbances as the calorimetric signal $\dot{q}_{tot}$.

Additionally the reaction model complexity that can be identified by the method is rated: low for the evaluation methods I.A and I.B as only one step reactions can be identified. Medium for methods II.A and II.B as general reaction models can be evaluated but the information content of the evaluated calorimetric data is limited. High for methods III.B and III.C as additional, uncalibrated analytical information is included. Very high for method III.A as concentration measurements, based on a pre calibration of the chosen analytical technique, are included.

4. Conclusions

Several reaction calorimetric devices and measurement principles were discussed in the first part of this article. The discussion was restricted to isothermal measurements. However, the analysis of the heat-flow balances of the different reaction calorimeters clearly showed that even though the reaction temperature is controlled isothermally the dynamics of the measurement devices must be considered as the heat-flows as well as the temperature of the dynamic elements change during a reaction measurement. If such effects are neglected and the common steady-state isothermal heat-flow balances are applied, a time distorted total heat-flow rate might be determined. Different available devices and principles were therefore compared on the basis of their dynamic behavior.

Further, the different behavior of the calorimetric devices on a changing reactor-sided heat-transfer coefficient during a reaction measurement was demonstrated. Different calorimetric devices and techniques were listed that are less or not affected by this problem and consequently will deliver a more accurate calorimetric signal if the proper evaluation technique is used.

Once having determined a most accurate total heat-flow rate ($\dot{q}_{tot}$) during a reaction measurement, $\dot{q}_{tot}$ can be evaluated in order to determine the reaction enthalpy as well as the kinetics of the investigated reaction. In a second part of this article it was shown that the still widely used technique to integrate the calorimetric signal $\dot{q}_{tot}$ might be misleading as additional heat of mixing, heat of phase changes or measurement errors (time distortion, undetected heat-transfer changes, ambient temperature influences . . .) are integrated into the determined reaction enthalpy. If the integration of $\dot{q}_{tot}$ is further used to determine the rate constant of the reaction the same disturbances will also influence the determined rate constant. However more stable, model-based evaluation methods for the identification of the reaction enthalpy as well as the kinetic parameters were explained. Some of them can even be applied for complex multi-step reactions as additional analytical data is included into the evaluation. Especially if concentration measurements, carried out with a pre calibrated analytical device, such as a HPLC, GC, or spectrometer, are included.

Because the reaction calorimetric signal represents a differential kinetic signal it is well suited to be combined with an additional integral kinetic signal (IR, Raman, UV-Vis, NIR spectra, concentrations measurements . . .) to achieve an even more robust evaluation. Possible combined

evaluation methods were also listed in the second part of this article.

5. Outlook

Up to now reaction calorimetry is barely used in synthesis laboratories where reactions and process procedures are initiated. As shown, several different reaction calorimetric devices (sample volume, accuracy, temperature range ...) are available on the market. It seems only a question of time until appropriate devices will also appear in a synthesis lab and replace the regular glass ware. Not only the temperature control, pressure resistance as well as the stirring will improve but reaction calorimetry could also introduce a process view already in early stages of process development—even if the measured reaction heat-flow rate is only used as a qualitative reaction profile. This could lead in the very early development phase of a chemical process to more data oriented laboratory procedures and a faster and more systematic reaction optimization and process scale-up.

References

[1] C. Guntern, A.H. Keller, K. Hungerbühler, Ind. Eng. Chem. Res. 37 (1998) 4017–4022.
[2] O. Levenspiel, Chemical Reaction Engineering, third ed., 1998.
[3] A. Zogg, A Combined Approach using Calorimetry and IR-ATR Spectroscopy for the Determination of Kinetic and Thermodynamic Reaction Parameters, Discussion ETH No. 15086, ETH Zürich, ETH Zürich, http://www.e-collection.ethbib.ethz.ch/cgi-bin/show.pl?type=diss&nr=15086, 2003.
[4] F. Becker, Chem. Ing. Tech. 19 (1968) 933–980.
[5] L.G. Karlsen, J. Villadsen, Chem. Eng. Sci. 42 (1987) 1153–1164.
[6] R.N. Landau, Thermochim. Acta 289 (1996) 101–126.
[7] W. Regenass, Chimia 51 (1997) 189–200.
[8] W. Hemminger, G. Höhne, Calorimetry: Fundamentals and Practice, Verlag Chemie, Weinheim, 1984.
[9] W. Regenass, in: Proceedings of the Second Symposium der Gesellschaft für Thermische Analyse, 1976.
[10] H. Martin, Wärmeflusskalorimetrie unter präparativen Bedingungen und ihre Anwendung zur Verfolgung der Isomerisierungskinetik von Trimethylphosphit, Ph.D. Thesis, University of Basel, Basel, 1975.
[11] Mettler Toledo, http://www.mt.com.
[12] R. Riesen, B. Grob, Swiss Chem. 7 (1985) 39–43.
[13] Systag, http://www.systag.ch.
[14] HEL, http://www.helgroup.co.uk.
[15] J. Singh, Process Saf. Prog. 16 (1997) 43–49.
[16] H.M. Andersen, J. Polym. Sci. Part A-1 4 (1966) 783–791.
[17] H.M. Andersen, J. Polym. Sci. Part A-1 7 (1969) 2889–2896.
[18] W. Köhler, O. Riedel, H. Scherer, Chem. Ing. Tech. 44 (1972) 1216–1218.
[19] B. Hentschel, Chem. Ing. Tech. 51 (1979) 823.
[20] J. Schildknecht, Thermochim. Acta 49 (1981) 87–100.
[21] M. Pollard, Org. Process Res. Dev. 5 (2001) 273–282.
[22] J. Pastré, A. Zogg, U. Fischer, K. Hungerbühler, Org. Process Res. Dev. 5 (2001) 158–166.
[23] C. Simms, J. Singh, Org. Process Res. Dev. 4 (2000) 554–562.
[24] M.R. Meeks, Polym. Eng. Sci. 9 (1968) 141–151.
[25] Chemisens, http://www.chemisens.com.
[26] Zeton-Altamira, http://www.zetonaltamira.com.
[27] W. Pauer, J.P. Tchonkou, H.U. Moritz, D. Brown, Workshop Reaktionskalorimetrie, 1999.
[28] F. Becker, W. Walisch, Z. Phys. Chem. 46 (1965) 279–293.
[29] H. Nilsson, C. Solvegren, B. Törnell, Chem. Scr. 19 (1982) 164–171.
[30] H. Nilsson, C. Silvegren, B. Törnell, Die Angew. Makromol.Chem. 112 (1983) 125–142.
[31] L. Jansson, H. Nilsson, C. Silvegren, B. Törnell, Thermochim. Acta 118 (1987) 97–105.
[32] M. Zogg, Einführung in die Mechanische Verfahrenstechnik, third ed., B.G. Teubner, Stuttgart, 1993.
[33] V.D.I. Wärmeatlas, eighth ed., Springer, Düsseldorf, 1997.
[34] L.G. Karlsen, J. Villadsen, Chem. Eng. Sci. 42 (1987) 1165–1173.
[35] J.M. Zaldívar, H. Hernández, C. Barcons, Thermochim. Acta 289 (1996) 267–302.
[36] RC1 Handbook, ed. 01/08, Mettler-Toledo GmbH, Switzerland, 2001.
[37] E. Cesari, P.C. Gravelle, J. Gutenbaum, J. Hatt, J. Navarro, J.L. Petit, R. Point, V. Torra, E. Utzig, W. Zielenkiewicz, J. Therm. Anal. 20 (1981) 47–59.
[38] L. Vincent, N. Sbirrazzuoli, S. Vyazovkin, Ind. Eng. Chem. Res. 41 (2002) 6650–6655.
[39] W. Regenass, Chimia 37 (1983) 430–437.
[40] A. Zogg, U. Fischer, K. Hungerbühler, Ind. Eng. Chem. Res. 42 (2003) 767–776.
[41] B. Baranek, M. Gottfried, K. Korfhage, W. Pauer, K. Schulz, H.U. Moritz, Mettler Toledo Publication, 1999.
[42] W. Litz, J. Therm. Anal. 27 (1983) 215–228.
[43] M. Schlegel, A. Löwe, Chem. Eng. Process. 37 (1997) 61–67.
[44] J. Schildknecht, in: Proceeding of the Second International Symposium on Loss Prevention and Safety Promotion in the Process Industries III, 1977, pp. 139–143.
[45] A. Tietze, A. Pross, K.H. Reichert, Chem. Ing. Tech. 68 (1996) 97–100.
[46] S. BenAmor, D. Colombié, T. McKenna, Ind. Eng. Chem. Res. 41 (2002) 4233–4241.
[47] A. Zogg, M. Wohlwend, U. Fischer, K. Hungerbühler, Patent: Kalorimeter, No. EP 1184649, Application No. 00810797.1, 2000.
[48] T. Stockhausen, J. Prüss, H.-U. Moritz, Dechema-Monographien 127 (1992) 341–349.
[49] S. Erwin, K. Schulz, H.U. Moritz, C. Schwede, H. Kerber, Chem. Eng. Technol. 24 (2001) 305–311.
[50] Setaram, http://www.setaram.com.
[51] R. André, L. Bou-Diab, P. Lerena, F. Stoessel, M. Giordano, C. Mathonat, Org. Process Res. Dev. 6 (2002) 915–921.
[52] Safety series, Drying of Solids, second ed., booklet 6, ESCIS Basel, Switzerland, 2003.
[53] G.D. Domenico, G. Maschio, D.G. Lister, A. Stassi, Rivista Dei Combustibili 55 (2001) 292–298.
[54] F. Becker, A. Maelicke, Z. Phys. Chem. 55 (1967) 280–295.
[55] O. Ubrich, B. Srinivasan, P. Lerena, D. Bonvin, F. Stoessel, J. Loss Prev. Process Ind. 12 (1999) 485–493.
[56] C. LeBlond, J. Wang, R.D. Larsen, C.J. Orella, A.L. Forman, R.N. Landau, J. Laquidara, J.R. Sowa, D.G. Blackmond, Q.K. Sun, Thermochim. Acta 289 (1996) 189–207.
[57] F. Stoessel, J. Therm. Anal. 49 (1997) 1677–1688.
[58] W. Litz, J. Therm. Anal. 32 (1987) 1991–1999.
[59] J. Snee, C. Bassani, J.A.M. Ligthart, J. Loss Prev. Process Ind. 5 (1993) 87–93.
[60] C.F. Pinto Machado e Silva, J.F. Cajaiba da Silva, Org. Process Res. Dev. 6 (2002) 829–832.
[61] A. Crevatin, F. Mascarello, B. Leuthe, B. Minder, I. Kikic, Ind. Eng. Chem. Res. 38 (1999) 4629–4633.
[62] R.N. Landau, D.G. Blackmond, H.H. Tung, Ind. Eng. Chem. Res. 33 (1994) 814–820.
[63] W. Köhler, O. Riedel, H. Scherer, Chem. Ing. Tech. 45 (1973) 1289–1294.
[64] W. Walisch, F. Becker, Z. Phys. Chem. 46 (1965) 268–278.

[65] R.M. Landau, U. Singh, F. Gortsema, Y. Sun, S.C. Gomolka, T. Lam, M. Futran, D.G. Blackmond, J. Catal. 157 (1995) 201–208.
[66] A. Lunghi, M.A. Alos, L. Gigante, J. Feixas, E. Sironi, J.A. Feliu, P. Cardillo, Org. Process Res. Dev. 6 (2002) 926–932.
[67] BatchCAD, Hyprotech, http://www.hyprotech.com/batchcad.
[68] N. Sbirrazzuoli, L. Vincent, S. Vyazovkin, Chemom. Intell. Lab. Syst. 54 (2000) 53–60.
[69] J.J.P. Stewart, MOPAC, Fujitsu Ltd., http://www.schrodinger.com/Products/mopac.html.
[70] F.W. Evans, H. Frey, Chimia 34 (1980) 247–249.
[71] H.L. Anderson, A. Kemmler, R. Strey, J. Therm. Anal. 47 (1996) 543–557.
[72] B. Hinz, K. Heldt, H.L. Anderson, Thermochim. Acta 310 (1998) 95–99.
[73] K. Heldt, H.L. Anderson, B. Hinz, Thermochim. Acta 310 (1998) 179–184.
[74] T. Willms, H.L. Anderson, K. Heldt, B. Hinz, Thermochim. Acta 310 (1998) 141–145.
[75] ACSL Optimize, Aegis Technologies Group, Inc., http://www.acslsim.com.
[76] U.C. Dyer, D.A. Henderson, M.B. Mitchel, P.D. Tiffin, Org. Process Res. Dev. 6 (2002) 311–316.
[77] L. Balland, L. Estel, J.M. Cosmao, N. Mouhab, Chemom. Intell. Lab. Syst. 50 (2000) 121–135.
[78] BatchReactor, ProSim, http://www.prosim.com.
[79] ChemCad, http://www.chemstations.net.
[80] A. Zogg, U. Fischer, K. Hungerbühler, Chem. Eng. Sci., 2003, submitted.
[81] R.M. Machado, J.W. Mitchell, J.P. Bullock, B.E. Farrell, Thermochim. Acta 289 (1996) 177–187.
[82] B. Fillion, B.I. Morsi, K.R. Heier, R.M. Machado, Ind. Eng. Chem. Res. 41 (2002) 697–709.
[83] J. Sempere, R. Nomen, J.L. Rodriguez, M. Papadaki, Chem. Eng. Process. 37 (1998) 33–46.
[84] C. LeBlond, J. Wang, R. Larsen, C. Orella, Y.K. Sun, Top. Catal. 5 (1998) 149–158.
[85] A. Zogg, U. Fischer, K. Hungerbühler, Chemom. Intell. Lab. Syst., 2004 accepted.
[86] R.N. Landau, R.F. McKenzie, A.L. Forman, R.R. Dauer, M. Futran, A.D. Epstein, Process Control Qual. 7 (1995) 133–142.
[87] D.J. am Ende, P.J. Clifford, D.M. De Antonis, C. Santa Maria, S.J. Bernek, Org. Process Res. Dev. 3 (1999) 319–329.
[88] R. Nomen, J. Sempere, K. Avilés, Chem. Eng. Sci. 56 (2001) 6577–6588.